

## NUMERICAL MODELING OF DYNAMIC COMPACTION IN DRY SAND USING DIFFERENT CONSTITUTIVE MODELS

M. Pourjenabi<sup>1</sup>, E. Ghanbari<sup>2</sup>, and A. Hamidi<sup>3\*</sup>

<sup>1</sup>Kharazmi University  
P.O.Box 15614, Tehran, Iran  
m.pourjenabi@khu.ac.ir

<sup>2</sup>Kharazmi University  
P.O.Box 15614, Tehran, Iran  
std\_ghanbari@khu.ac.ir

<sup>3</sup>Kharazmi University  
P.O.Box 15614, Tehran, Iran  
hamidi@khu.ac.ir

**Keywords:** Dynamic compaction, constitutive model, numerical modeling, cap plasticity, Mohr-Coulomb.

**Abstract.** *Dynamic compaction is a useful method of soil improvement for loose sands. In this method a tamper falls down from a specified height on the soil in order to reach the desired compaction depth. The method is invented and introduced by Louis Menard and applied at Nice airport in France. It has been developed and progressed afterward and has been used in several projects for land reclamation.*

*Numerical modeling is a useful tool for simulation of dynamic phenomena in geotechnical engineering. Several researchers have worked on numerical simulation of dynamic compaction using different codes and implemented solutions for prediction of appropriate patterns of compaction. However, less attention has been paid to the effect of different constitutive models applied in numerical solution.*

*In present research, ABAQUS 6.10-1 software is used for two dimensional modeling of dynamic compaction operation in dry sand. The program is able to simulate process of dynamic compaction with high acquisition. Cap plasticity critical state model besides Mohr-Coulomb failure criterion are used in numerical simulation and the effect of these constitutive models are investigated on the peak particle velocity and peak ground acceleration besides the crater depth.*

*Results of comparison indicated that application of different constitutive models influences the numerical simulation of the phenomenon. Implementation of cap plasticity model results in better prediction of crater depth and variations of relative density in depth compared to the Mohr-Coulomb failure criterion.*

## 1 INTRODUCTION

Dynamic compaction is a useful method for compacting granular soils which has first been introduced by Menard in 1975. This method is based on falling a tamper (weighting from 5 to 40 tons) from height of 15 to 30 meters on the loose sand that results in desirable compaction and increases the shear strength of base soil.

Many researchers have used numerical or physical modeling to study this phenomenon [1-8] and others have studied the results of dynamic compaction in the field [9-18]. In addition, analytical methods have been used for surveying different parameters of this method [19-22].

In numerical modeling process, it is very important to utilize a proper constitutive model for the soil in order to predict its behavior in a good manner. Unlike the behavior of soils in triaxial tests or failure of the soil under foundations, that the increase in axial stress has an important role in failure, increase in confining stress results in failure of soil during dynamic compaction.

Mohr-Coulomb criterion assumes that failure occurs when shear stress on any point in a material reaches a certain value that depends linearly on normal stress in the same plane [4]. Unlike Drucker-Prager criterion, Mohr-coulomb criterion assumes that failure of typical geotechnical materials generally includes some small dependence on the intermediate principal stress. Mohr-Coulomb constitutive model has been used for simulating dynamic compaction in finite element code ABAQUS [4]. Cap-plasticity models have also been used by a number of researchers for simulation of dynamic compaction in granular materials [24-26].

In this paper, a two dimensional model in finite element code ABAQUS is used to survey the differences between cap-plasticity and Mohr-Coulomb constitutive models. Results are compared with an experimental centrifuge test [7].

## 2 CONSTITUTIVE MODELS USED IN THE NUMERICAL ANALYSIS.

In present study, numerical analysis has been performed using two different constitutive models, i.e. Mohr-Coulomb and cap plasticity model.

### 2.1 Mohr-Coulomb model

Mohr-coulomb model is defined in  $\tau$ - $\sigma$  plane. In this model, shear strength increases with enhancement of normal stress on the failure plane:

$$\tau = c + \sigma \tan \phi \quad (1)$$

$\tau$  is the shear stress,  $c$  is the cohesion of material,  $\phi$  is the material friction angle and  $\sigma$  is the normal stress. Mohr-Coulomb failure criterion in  $\Pi$  plane is shown in Fig. 1.

According to this criterion, yield strength in compression is higher than that in extension. It shows the dependence of the behavior on the third invariant of the stress tensor. The criterion is expressed in terms of maximum and minimum principal stresses, and hence does not incorporate the effects of the intermediate principal stresses [27].

### 2.2 Cap plasticity model

The model predicts hardening behavior of soil and is useful for application in dynamic problems. Cap models particularly are used to predict the behavior of soils under impact loads [25, 28]. Also cap plasticity model with a linear shear yield surface has been used for modeling dynamic compaction process in granular soils [1]. In this study, similar cap plasticity model has been used. Figure 2 indicates yield criterion of the model in the first and second

stress invariants space,  $(J_1 - \sqrt{J_{2D}})$ . The model has two different yield surfaces to consider soil hardening during shear and isotropic loading. First one is a linear shear yield surface based on Drucker-Prager yield criterion in Eq. 2 and is fixed. The second one is a moving cap that is defined by Eq. 3 and is used to express soil failure under isotropic effective stress.

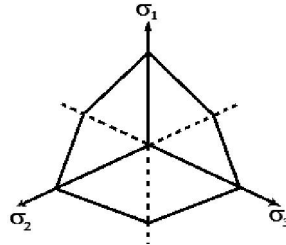


Figure 1: Mohr-Coulomb criterion in  $\Pi$ plane

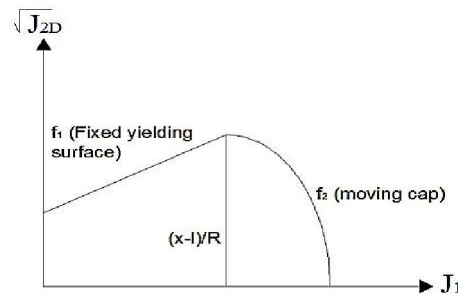


Figure2: Yield surface of the cap model in stress space.

$$f_1 = \sqrt{J_{2D}} - \alpha j_1 - \kappa = 0 \quad (2)$$

$$f_2 = (J_1 - 1)^2 + R^2 J_{2D} - (X - l)^2 = 0 \quad (3)$$

$$l = \frac{X - R\kappa}{1 + \alpha R} \quad (4)$$

$\alpha$  and  $\kappa$  are constants of Drucker-Prager failure criterion.  $X$  is the hardening parameter;  $R$  is the material parameter and  $l$  is the first invariant of stress tensor at the intersection point of the fixed yield surface and the moving cap. Cap is extended due to the soil hardening based on plastic volumetric strain in every step and is defined according to Eq.5.

$$X = -\frac{1}{D} \text{Ln} \left( 1 - \frac{\epsilon_v^p}{W} \right) + X_0 \quad (5)$$

Here,  $W$  and  $D$  are material parameters and  $X_0$  is initial stresses due to gravity analysis.

### 3 NUMERICAL MODELING

Two dimensional axisymmetric model has been developed using ABAQUS as shown in Fig. 3. Compaction is performed using a 20 ton poulder falling from 20m height. Model height and width are 18m and 14m respectively. Also the number of impacts is considered 5 and 10 blows in the analysis. Features of poulder and soil parameters in two cases of Mohr-coulomb and cap plasticity models are shown in Tables 1 and 2 [7].

Interface elements have been used to define the contact between tamper and the ground surface. Friction coefficient is taken 0.5 for contact property. Total time for each impact is 60sec and minimum increment of time is  $10^{-8}$ sec that is properly small for dynamic and specially impact problems. Large deformation condition is also considered in this model.

In the first step, gravity analysis is performed to exert initial stresses, also at the end of each step, void ratio is obtained by substituting volumetric strain in Eq.6.

$$e = e_0 - (1 + e_0)\varepsilon_v \quad (6)$$

Where  $e_0$  is the initial void ratio and  $\varepsilon_v$  is volumetric plastic strain. Also  $e$  is void ratio at the end of each step. Soil density at the end of each step is calculated from Eq.7. Hence, by applying maximum and minimum void ratios in Eq. 8, relative density and its rate of increase can be determined.

$$\gamma = \frac{G_s \gamma_w}{1+e} \quad (7)$$

$$Dr = \frac{e_{max} - e}{e_{max} - e_{min}} \quad (8)$$

Here,  $e_{max}$  and  $e_{min}$  are 0.86 and 0.51, respectively. Also bulk modulus is reassigned through Eq.9 considering the role of change in relative density and mean effective stress in different soil layers. Applying bulk modulus in Eq.11, elasticity modulus is achieved in each step.

$$k = k_r P_a \left(\frac{\bar{p}}{P_a}\right)^{0.5} \quad (9)$$

$$k_r = \beta \exp(\gamma \cdot Dr) \quad (10)$$

$$E = 3(1 - 2\vartheta)K \quad (11)$$

Here,  $K$  is the bulk modulus,  $\bar{p}$  is the mean effective stress,  $Dr$  is the relative density,  $P_a$  is atmospheric pressure,  $\beta$  and  $\gamma$  are 120 and 0.0134 respectively and  $\vartheta$  is the poisson's ratio.

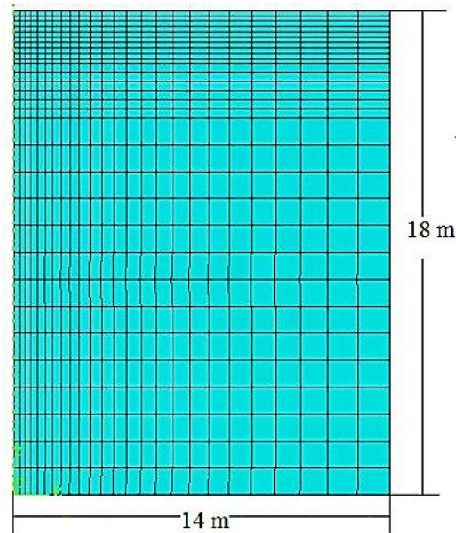


Figure 3: Dimensions and mesh of the model

Parameters	Value
Tamper weight	25 ton
Falling height	20 meter
Tamper cross section area	4.5 m <sup>2</sup>
Elasticity modulus	90GPa
Poisson's ratio	0.2

Table 1: Tamper parameters

Parameters	Value
Internal friction angle	29.9 degree
Dilation angle	10 degree
Cohesion	0
Soil density	15.7 kN/m <sup>3</sup>
Young modulus	25 MPa
Poisson's ratio	0.25
Damping constants( $\eta_1, \eta_2$ )	0,0.01
R	4.33
W	0.4
D	$18 \times 10^{-5}$ (m <sup>2</sup> /kN)

Table 2: Soil parameters

#### 4 NUMERICAL MODELING RESULTS

Centrifuge tests have been used to simulate dynamic compaction process and the results have been represented in different conditions of impact [7]. Initial relative density of soil was 35%. Contours of increase in relative density in soil for 5 and 10 blows are represented in Figs.4-a and 4-b. As shown in Fig. 4-a, crater depth in 5blows, is about 1.2 meter. Also 40%, 20% and 10% increase in relative density induced in 3.2, 4.2 and 5.2 meters depth respectively. Fig4-b represents similar contours for 10 blows. It can be observed that the crater depth in 10 blows is recorded as 1.5 meters and 40%, 20% and 10% increase in relative density induced in 4.55, 5.6 and 6.35meters depth respectively.

Figs 5-a and 5-b shows the results of numerical analysis using cap plasticity model for 5 and 10 blows respectively. Crater depth for 5blows is 1.27 meter and 40%, 20% and 10% increase in relative density occurred in 2.7, 3.45 and 4.8 meters depth. Based on Fig. 5-b, crater depth for 10blows is 2.12 meter and 40%, 20% and 10% increase in relative density occurred in 3.6, 4.85 and 6.32 meters depth.

Figs.6-a and 6-b indicate the results of numerical analysis using Mohr-Coulomb failure criterion for 5 and 10blows respectively. Fig. 6-a shows the contours and crater depth for 5blows. It can be observed that crater depth is 0.275 meters and contours of 40%, 20% and 10% relative density are in 2.2, 3.11 and 3.67 meters depth. Based on Fig. 6-b, crater depth in 10blows is 0.377 meters and the depth associated to 40%, 20% and 10% increase in relative density are 3.2, 3.62 and 4 meters respectively.

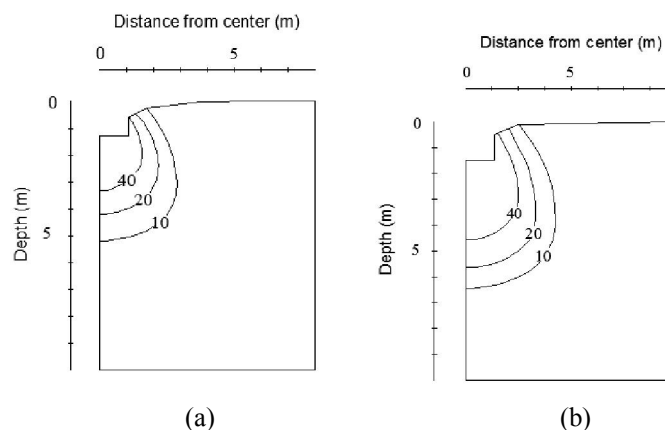


Figure 4: Results of centrifuge test reported by Oshima and Takada [7] for (a) 5blows (b) 10blows

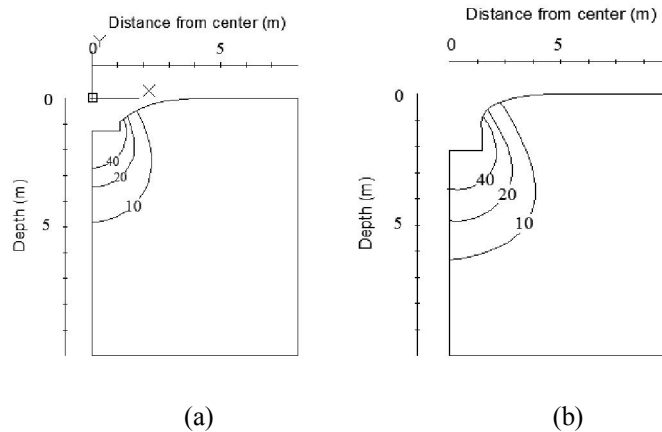


Figure 5: Results of numerical analysis using cap plasticity model for (a) 5blows (b)10blows

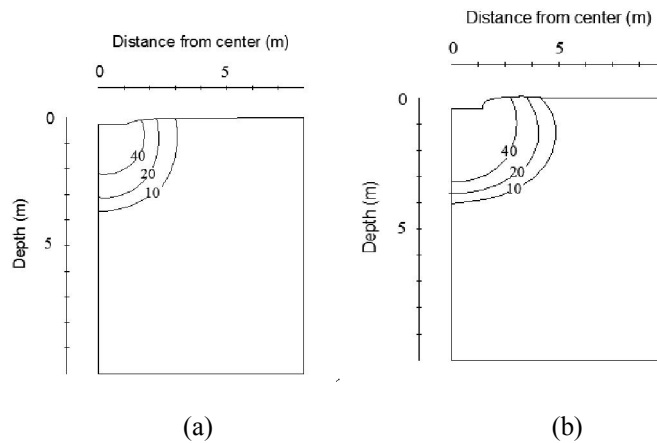


Figure6: Results of numerical analysis using Mohr-Coulomb model for (a) 5 blows (b) 10 blows

It is obvious from the figures that dynamic compaction process modeling using Mohr-Coulomb failure criterion results in lower crater depth and higher depth of relative density contours. It is due to the soil dilation after each impact which occurs using Mohr-Coulomb model which is not able to predict failure during compressive loading of confinement. On the contrary, modeling the soil behavior using cap plasticity model results is a higher crater depth and relative density contours which are more consistent with centrifuge model test results.

Figure 7 shows the variation of crater depth with time for two applied models. It is visible that crater depth in Mohr-Coulomb model is much lower than the other one. Also at the end of each impact there is an unusual increase in volume of the soil which has not occurred for cap plasticity model. As a result, Mohr-Coulomb failure criterion is not applicable for prediction of dynamic compaction in numerical analysis.

## 5 CONCLUSION

A two dimensional axisymmetric model was developed for simulation of dynamic compaction process using finite element code ABAQUS applying Mohr-Coulomb and cap plasticity models. Results are compared with a physical centrifuge mode and the following conclusions are made:

- Cap plasticity constitutive model is suitable for predicting dynamic compaction process because of its moving cap which enables the model to incorporate soil hardening during isotropic compression and confinement.
- Using Mohr-Coulomb failure criterion, the soil expands after each impact. The value of dilation angle affects this dilative behavior. As a result, this model results in lower volumetric strains and less crater depth besides more depth of relative density contours compared to the model tests. It can be concluded that Mohr-Coulomb criterion is not a suitable model for prediction of dynamic compaction process.

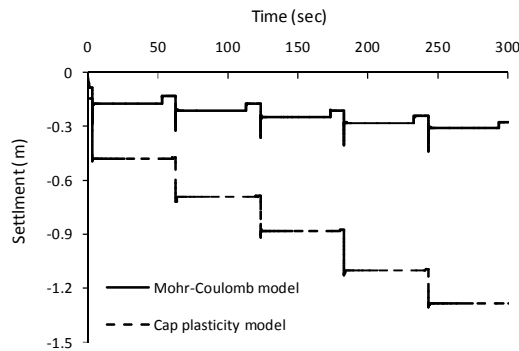


Figure 7: Variation of crater depth versus time for Mohr-Coulomb and cap plasticity models

## 6 REFERENCES

- [1] A. Ghassemi, A. Pak, H. Shahir, Numerical study of the coupled hydro-mechanical effects in dynamic compaction of saturated granular soils. *Computers and Geotechnics*, **37**, 10–24, 2010.
- [2] G. Jahangiri, A. Pak, A. Ghassemi, A novel numerical method for determination of print spacing in dynamic compaction operation of dry sand. *4<sup>th</sup> International Conference on Geotechnical Engineering and Soil Mechanics*, Tehran, Iran, 2010.
- [3] M. Jia, J. Zhou, Investigation of mechanical response induced in dynamic compaction of sandy soils with PFC2D. *GeoShanghai International Conference*, Shanghai, China, 2010.
- [4] J.L. Pan, A.R. Selby, Simulation of dynamic compaction of loose granular soils. *Advances in Engineering Software*, **33**, 631–640, 2002.
- [5] W. Li, Q. Gu, L. Su, B. Yang, Finite element analysis of dynamic compaction in soft foundation. *Procedia Engineering*, **12**, 224–228, 2011.
- [6] O.P. Minaev, Effective method for dynamic compaction of slightly cohesive saturated soils. *Soil Mechanics and Foundation Engineering*, **39**, 208-213, 2002.
- [7] A. Oshima, N. Takada, Relation between compacted area and ram momentum by heavy tamping. *14<sup>th</sup> International Conference on Soil Mechanics and Foundation Engineering*, Hamburg, Germany, 1997.
- [8] F. Jafarzadeh, Dynamic compaction method in physical model test. *Scientia Iranica*, **13**, 187-192, 2006.
- [9] H. Arslan, G. Baykal, O. Ertas, Influence of tamper weight shape on dynamic compaction. *Ground Improvement*, **11**, 61–66, 2007.
- [10] S.J. Feng, W.H. Shui, W.H. Gao, L.J. He, K. Tan, Field evaluation of dynamic compaction on granular deposits. *Performance of Constructed Facilities*, **25**, 241-249, 2010.

- [11] L.J. Hua, Y.J. Bo, X. Hu, C. Wei, Dynamic compaction treatment technology research of red clay soil embankment in southern mountains. *Journal of Central South University of Technology*, **15**, 50–57, 2006.
- [12] J.H. Hwang, T.Y. Tu, Ground vibration due to dynamic compaction. *Soil Dynamics and Earthquake Engineering*, **26**, 337–346, 2006.
- [13] F. Kopf, I. Paulmich, D. Adam, Modelling and simulation of heavy tamping dynamic response of the ground. *14<sup>th</sup> Danube-European Conference on Geotechnical Engineering*, Bratislava, Slovak Republic, 2010.
- [14] L. Menard, Y. Broise, Theoretical and practical aspects of dynamic consolidation. *Geotechnique*, **25**, 3-16, 1975.
- [15] P.W. Mayne, J.S. Jones, Impact stresses during dynamic compaction. *Geotechnical Engineering*, **109**, 1342-1346, 1983.
- [16] P.W. Mayne, J.S. Jones, J.C. Dumas, Ground response to dynamic compaction. *Geotechnical Engineering*, **110**, 757-774, 1984.
- [17] K.M. Rollins, J. Kim, Dynamic compaction of collapsible soils based on U.S. case histories. *Geotechnical and Geoenvironmental Engineering*, **136**, 1178-1186, 2010.
- [18] W.L. Zou, Z. Wang, Z.F. Yao, Effect of dynamic compaction on placement of high-road embankment. *Performance of Constructed Facilities*, **19**, 316-323, 2005.
- [19] Y.K. Chow, D.M. Yong, K.Y. Yong, S.L. Lee, Monitoring of dynamic compaction by deceleration measurements. *Computers and Geotechnics*, **10**, 189-209, 1990.
- [20] Y.K. Chow, D.M. Yong, K.Y. Yong, S.L. Lee, Dynamic compaction analysis. *Geotechnical Engineering*, **118**, 1141-1157, 1992.
- [21] Y.K. Chow, D.M. Yong, K.Y. Yong, S.L. Lee, Dynamic compaction of loose granular soils: effect of print spacing. *Geotechnical Engineering*, **120**, 1115-1133, 1994.
- [22] J.M. Roesset, E. Kausel, V. Cuellar, J.L. Monte, J. Valerio, Impact of weight falling onto the ground. *Geotechnical Engineering*, **120**, 1394-1412, 1994.
- [23] R.G. Lukas, *Geotechnical engineering circular No. 1- Dynamic compaction*. FHWA-SA-95-037, 1995.
- [24] A. Pak, H. Shahir, A. Ghasemi, Behavior of dry and saturated soils under impact load during dynamic compaction. *16<sup>th</sup> International Conference on Soil Mechanics and Geotechnical Engineering*, Osaka, Japan, 2005.
- [25] Q. Gu, F.H. Lee, Ground response to dynamic compaction. *Geotechnique*, **52**, 481-93, 2002.
- [26] H.S. Thilakasiri, M. Qunaratne, G. Mullins, P. Stinnette, C. Kuo, Implementation aid for dynamic replacement of organic soils with sand. *Geotechnical and Geoenvironmental Engineering*, **127**, 25-35, 2001.
- [27] C.S. Desai, H.J., Siriwardane, *Constitutive laws for engineering materials, with emphasis on geologic materials*. Prentice Hall, 1984.
- [28] C.J. Poran, J. Rodriguez, A finite element analysis of impact behavior of sand. *Soils and Foundations*, **32**, 68–80, 1992.